Title

PMN-PT/Epoxy 1-3 composite based ultrasonic transducer for dual-modality photoacoustic and ultrasound endoscopy

Authors

Li, Yan
Lu, Gengxi
Chen, Jason J
et al.

Publication Date

2019-09-01

DOI

10.1016/j.pacs.2019.100138

Photoacoustics 15 (2019) 100138

Contents lists available at ScienceDirect

Photoacoustics

journal homepage: www.elsevier.com/locate/pacs

Research article

PMN-PT/Epoxy 1-3 composite based ultrasonic transducer for dual-modality photoacoustic and ultrasound endoscopy

Yan Li[a,c,1], Gengxi Lu[b,d,1], Jason J. Chen[a,c], Joseph C. Jing[a,c], Tiancheng Huo[a], Ruimin Chen[b], Laiming Jiang[d], Qifa Zhou[b,d], Zhongping Chen[a,c,*]

[a] Beckman Laser Institute, University of California, Irvine, Irvine, CA 92617, USA
[b] Department of Biomedical Engineering, Viterbi School of Engineering, University of Southern California, Los Angeles, CA 90089, USA
[c] Department of Biomedical Engineering, University of California, Irvine, Irvine, CA 92697, USA
[d] Roski Eye Institute, Keck School of Medicine, University of Southern California, Los Angeles, CA 90033, USA

ARTICLE INFO

Keywords:
Photoacoustic imaging
Ultrasound imaging
Endoscopic imaging
Gastrointestinal
Ultrasonic transducer
PMN-PT epoxy 1-3 composite
Composite based ultrasonic transducer

ABSTRACT

Endoscopic dual-modality photoacoustic (PA) and ultrasound (US) imaging has the capability of providing morphology and molecular information simultaneously. An ultrasonic transducer was applied for detecting PA signals and performing US imaging which determines the sensitivity and performance of a dual-modality PA/US system. In our study, a miniature single element 32-MHz lead magnesium niobate-lead titanate (PMN-PT) epoxy 1–3 composite based ultrasonic transducer was developed. A miniature endoscopic probe based on this transducer has been fabricated. Using the dual modality PA/US system with a PMN-PT/epoxy 1–3 composite based ultrasonic transducer, phantom and *in vivo* animal studies have been conducted to evaluate the performance. The preliminary results show enhanced bandwidths of the new ultrasonic transducer and improved signal-to-noise ratio of PA and US images of rat colorectal wall compared with PMN-PT and lead zirconate titanate (PZT) composite based ultrasonic transducers.

1. Introduction

Photoacoustic (PA) imaging is an emerging imaging modality that has been applied in a wide variety of biomedical applications, such as brain lesion detection and breast cancer diagnosis [1–3]. The advantage of PA imaging lies with its ability to reveal molecular information as biomolecules vary in absorption efficiency. In brief, PA imaging utilizes a non-ionizing nanosecond laser to deliver pulsed light into the biological tissue. When the pulsed laser energy is absorbed by the tissue sample, it is converted to heat which causes a transient thermoelastic expansion that emits wideband ultrasonic waves. A piezoelectric transducer or all-optical ultrasound (US) sensor can be used to detect these generated ultrasonic waves, or the PA signals. An all-optical US sensor, such as a Fabry-Pérot interferometer or microresonator, is able to provide wide detection bandwidth, resonance-free acoustic detection spectrum, and high resolution [4–11]. However, it still presents challenges for US detection. Chiefly, it requires a cost-intensive read-out system. In addition, with an all-optical US sensor, it is incapable of generating US waves to perform US imaging, which is often preferable in clinical applications. For the piezoelectric transducer, it can provide US detection with large penetration depth and high sensitivity. In addition, a piezoelectric transducer is able to emit and receive the US signal simultaneously. Therefore, integration with US imaging is seamless since PA imaging relies on the use of ultrasonic transducers. With the capability to simultaneously resolve molecular (PA) and structural information (US) in depth, dual-modality PA/US imaging has been used in various applications, including the detection of cancer and characterization of vulnerable plaque [12–20]. In our study, a piezoelectric transducer was applied for PA signal detection and to perform US imaging simultaneously.

The key factor of the performance of a PA/US imaging system is the ultrasonic transducer. For the PA/US transducer, the widely used materials include: lithium niobate ($LiNbO_3$) [21–23], lead magnesium niobate-lead titanate (PMN-PT) [17,24], and lead zirconate titanate (PZT) composite [12,13,15,25,26]. $LiNbO_3$, as the conventional single crystal, has stable and strong electro-mechanical coupling capabilities but exhibits inferior piezoelectric performance compared to PZT [27]. PZT is advantageous due to its high performance and ease of manufacture, yet it has a limited application in highly attenuative materials. Recently developed PMN-PT as a new class of signal-crystal

* Corresponding author at: Beckman Laser Institute, University of California, Irvine, Irvine, CA 92617, USA.
E-mail address: z2chen@uci.edu (Z. Chen).
[1] These authors contributed equally to this work.

https://doi.org/10.1016/j.pacs.2019.100138
Received 23 January 2019; Received in revised form 9 May 2019; Accepted 17 June 2019
Available online 20 June 2019

piezoelectric material has gained interest in the research field and has demonstrated improved piezoelectric performance. Its piezoelectric strain constant (d_{33}) ranging from 1500 to 2500 (pC/N) is approximately five times higher than that of PZT, and its electromechanical coupling coefficient k_t of ~0.58 is also superior [28,29]. In addition, it has been reported that the PMN-PT single crystal ultrasonic transducer shows improved performance over both PZT and PZT-based 1–3 composite ultrasonic transducers [30]. On top of PMN-PT's advantages, the PMN-PT/epoxy 1–3 composite material has further benefits. As one of the most promising in frontier transducer technology, piezoelectric rods embedded in a low-density polymer lower the acoustic impedance and highly enhance the electromechanical coupling coefficient. For the PMN-PT/epoxy 1-3 composite, the electromechanical coupling coefficient increases from 0.58 to 0.94, which inherently contributes to better acoustic impedance matching between transducers and water along with higher sensitivity and improved image resolution [31].

In this paper, we report on a 32-MHz single-element ultrasonic transducer with an aperture size of 0.5 mm fabricated using a PMN-PT/epoxy 1–3 composite. A miniature PA/US endoscopic probe (outer diameter: 1.45 mm) was fabricated based on this material for PA/US imaging. The manufacture process of the transducer, imaging probe design, and imaging system setup are described herein. The performance of the transducer was quantified using a reflector and tested in the rat gastrointestinal tract *in vivo*. The results demonstrated an enhanced sensitivity over conventional transducers.

2. Methods

2.1. Design and fabrication of the PMN-33%PT/epoxy 1–3 composite ultrasonic transducer

Fig. 1(a) illustrates the fabrication process of the PMN-PT/epoxy 1–3 composite. (1) A polished PMN-PT crystal plate was first diced along one direction using an automatic dicing saw (K&S 982-6, Kulicke and Soffa Industries, Inc.). (2) The kerfs were filled with epoxy (EPO-TEK 301, EPOXY Technology, Inc.). (3) After the epoxy was cured, the plate was diced again in the direction perpendicular to the kerfs. (4) The new kerfs were filled with the same epoxy and allowed to cure. (5) Lastly, the composite plate was flapped to the final thickness and coated with Cr/Au on both sides as electrodes. For endoscopic application, we fabricated an ultrasonic transducer with a $0.5 \times 0.5\ mm^2$ effective detection area, as shown in Fig. 1(b).

2.2. Imaging system setup

Fig. 2 shows the schematic of the dual-modality PA/US imaging system. A 532-nm nanosecond laser (Photonics Industries, DCH-532-10) with a repetition rate up to 300 kHz and a maximum power of 10 W was utilized for PA signal excitation. A condenser lens was used to couple the laser beam into a multimode fiber (MMF) then to a fiberoptic rotary joint. The rotary joint was powered by a rotary motor, and a motorized linear translation stage was incorporated to allow spiral scanning for volumetric imaging. In the imaging probe, the laser beam was propagated through the MMF, focused by a 0.5 mm gradient index (GRIN) lens, and reflected towards the tissue surface by a rod mirror with a diameter of 0.5 mm at an angle of 40°. The aforementioned 32-MHz center frequency PMN-PT/epoxy 1–3 composite ultrasonic transducer was aligned with the optical components and housed in a metal cap. The transducer was tilted 10-degrees toward the rod mirror in order to obtain optimal overlap between the laser beam and the acoustic beam at the desired imaging depth (1.5–4.5 mm). A torque coil connecting the metal cap and the fiberoptic rotary joint was used to protect the MMF and to transmit the rotational torque produced by the rotary joint. An electrical slip ring (Hangzhou Prosper Mechanical & Electrical Technology Co., Ltd) was integrated with the imaging probe to maintain the transmission of the US signal during rotation. To co-register the PA and US, the trigger signal from a nanosecond laser was used to synchronize laser emission, data acquisition, and pulse-echo US emission. Since a single ultrasonic transducer was used for both PA signal detection and US signal emission/detection, the US pulse echo emission was delayed by ~5 μs from the trigger (Fig. 2). Both the PA and US signals were detected by the same ultrasonic transducer, amplified by the pulse receiver (Olympus Corp., 5073PR), and digitized with a data acquisition (DAQ) card in a computer. During imaging, the probe was rotated at 20 revolutions per second (RPS) while simultaneously pulled back *via* the translation stage for volumetric PA/US imaging.

2.3. Imaging protocol

The animal study was performed on Sprague Dawley (SD) rats. Before the experiment, a rat was placed in a closed plexiglass chamber for general anesthesia induction, and then removed from the chamber for an intraperitoneal injection of ketamine hydrochloride (87 mg/kg) and xylazine (10 mg/kg). After the rat was anesthetized, an enema was performed. After that, an optically and ultrasonically transparent tube (material: Pebax®; wall thickness: 0.005") was inserted to inflate the rectum wall, and the probe was inserted into the tube for imaging. All procedures were reviewed and approved by the Institutional Animal Care and Use Committee at the University of California, Irvine under protocol #2016-3198.

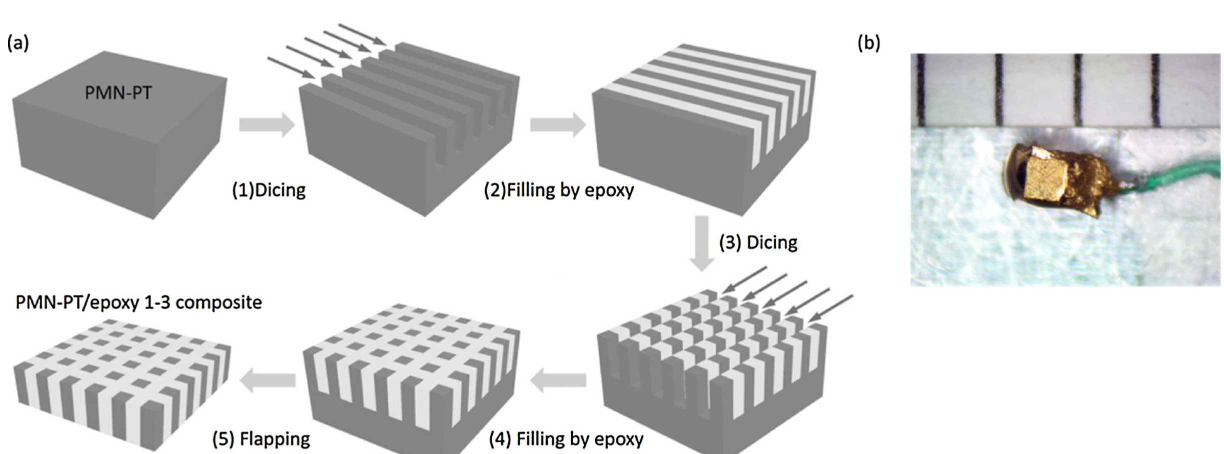

Fig. 1. PMN-PT/epoxy 1–3 composite ultrasonic transducer. (a) Fabrication process of PMN-PT/epoxy 1–3 composite material. (b) Photo of ultrasonic transducer.

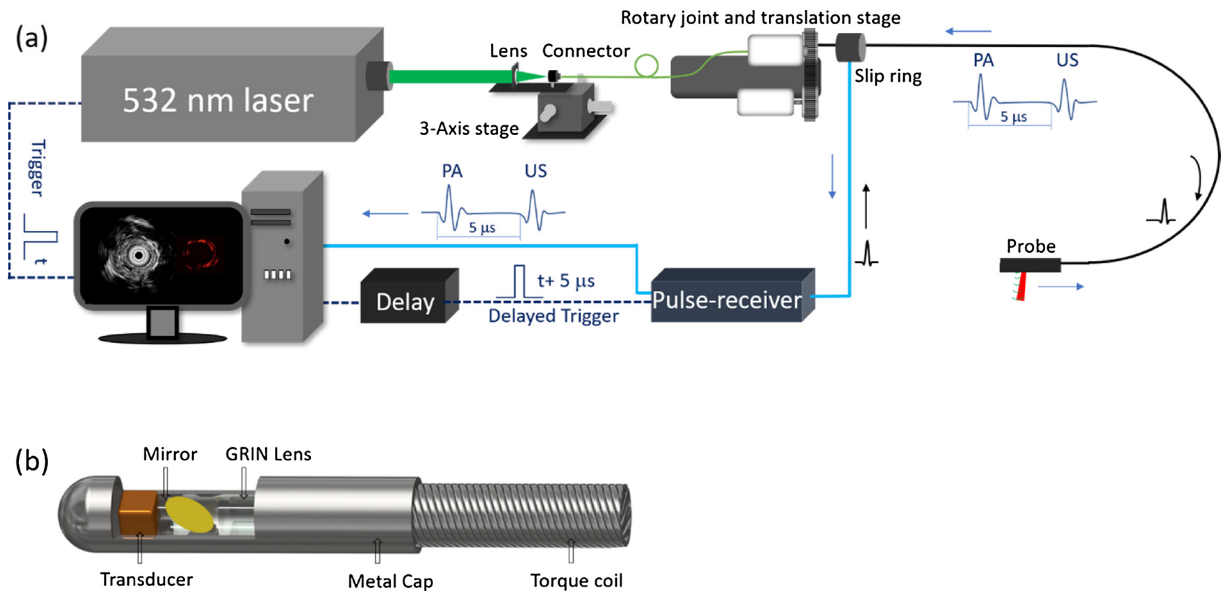

Fig. 2. Setup of the dual-modality PA and US imaging system. (a) Schematic of the imaging system. (b) Schematic of the imaging probe.

3. Results

3.1. Performance of ultrasonic transducers

A glass mirror was used as an imaging target in the pulse-echo test to measure the frequency spectrum of three representative ultrasonic transducers made of PMN-PT/epoxy 1–3 composite, PMN-PT, and PZT composite (Fig. 3). In Fig. 3, the blue curves represent the pulse-echoes of the ultrasonic transducers, and the red curves show the frequency responses. In the plot, the pulse echo on the left is the initial pulse from the ultrasonic transducer, and the one on the right is the US signal from the mirror. As shown in Fig. 3, the PMN-PT-based transducer has a center frequency of around 35 MHz and a 78% frequency bandwidth (at -6 dB), and those of the PZT composite based transducer are 40 MHz and 47%, respectively. In contrast, the transducer made of the PMN-PT/epoxy 1–3 composite material has a center frequency at 32 MHz with a 91% bandwidth, which shows a better electro–mechanical performance compared with the other two ultrasonic transducers. The characterizations of the three types of ultrasounic transducers, including the center frequency, bandwidth, signal-to-noise ratio (SNR), and insert loss, are shown in Table 1.

3.2. Comparison of US and PA images

Imaging probes were fabricated using each of the transducers, and the SD rats were imaged with each of the probes (Fig. 4). The representative US and PA images from PMN-PT/epoxy 1–3 composite, PMN-PT, and PZT composite, respectively, are shown in Fig. 4. The SNRs of US and PA are reported in Table 2. The US images acquired using the probe made of PMN-PT/epoxy 1–3 composite demonstrate significant improvement in SNR compared to PMN-PT and PZT composite. This agrees with previously reported studies [30,31].

3.3. In vivo imaging of the rat rectum

To demonstrate its clinical application, *in vivo* imaging utilizing a PMN-PT/epoxy 1–3 composite PA/US probe was performed in the rectum of a SD rat. With a pullback speed of 1 mm/s using a motorized translation stage, 500 cross-sectional PA/US images were acquired sequentially. The representative images of different longitudinal positions are shown in Fig. 5. From the US images [Fig. 5(e–h)], the colorectal wall and the surrounding connective tissue can be identified throughthe

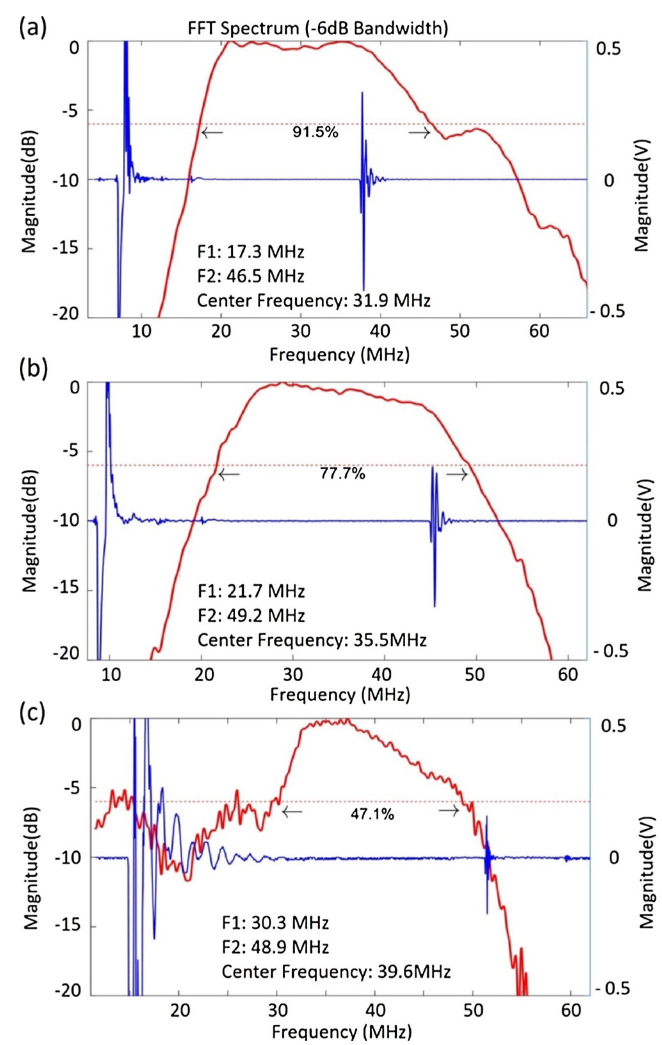

Fig. 3. Pulse-echo measurements and respective frequency spectra of different materials-based ultrasounic transducers. (a) PMN-PT/epoxy 1–3 composite, (b) PMN-PT, and (c) PZT composite. Blue curve: US pulse echo. Red curve: spectrum.

Table 1
Performance comparisons of PMN-PT/epoxy 1–3 composite, PMN-PT, and PZT composite transducers.

Material	Center Frequency (MHz)	Bandwidth (−6 dB)	SNR (dB)	Insert Loss (dB)	Noise equivalent pressure (Pa)
PMN-PT/epoxy 1-3 composite	31.9	91.50%	44.27	16	2.6
PMN-PT	35.5	77.70%	40.61	17	3
PZT composite	39.6	47.10%	30.8	21	1.7k

boundary delineated by the low intensity signal, indicated by the yellow dashed circle. In Fig. 5(a–d), the PA images show the depth-resolved blood vessel distribution, which is advantageous over the commonly used fluorescence imaging that lacks depth information. Co-registered images, shown in Fig. 5(i–l), provide helpful comprehensive information for lesion evaluation and is advantageous over either modality alone. Fig. 6 shows representative 3-dimensional (3D) PA and US images, respectively, of the rectum. The vasculature can be visualized in Fig. 6(a). The morphology of the rectum wall can be identified in Fig. 6(b) and (d).

Table 2
SNRs of PA and US images of *in vivo* imaging of rat rectum. The regions for SNR calculation are marked by green dashed boxes in Fig. 4.

Material	SNR (dB)	
	US	PA
PMN-PT/epoxy 1-3 composite	46.7	32.4
PMN-PT	32.2	31.8
PZT composite	33.4	31.5

4. Discussion

Endoscopic dual-modality PA/US imaging is a minimally invasive imaging modality that has the capability of visualizing the morphology and vasculature of the rectal wall. With the integration of a PMN-PT/epoxy 1–3 composite-based ultrasonic transducer which has been demonstrated to have high piezoelectric coefficients d_{33}, high coupling coefficients k_t, and low dielectric loss, we further improved the sensitivity of the conventional PA/US imaging system. The results obtained from the reflector and *in vivo* rat experiments have shown its enhanced sensitivity compared to the two conventional transducers (PMN-PT and PZT composite) based imaging systems. In the obtained PA/US images, the layered architecture and vasculature can be identified. With its small form factor (probe outer diameter < 1.5 mm), the multimodal imaging probe can access the colon through the accessory channel of a commercial endoscope, so it can be easily integrated into clinical practice to provide additional subsurface information.

Despite the superior performance of the PMN-PT composite, there are a few drawbacks. The first is the higher cost compared to conventional piezoelectric ceramics. However, the cost can be reduced with the development of new manufacturing methods. Another disadvantage of the PMN-PT composite is that its Curie temperature is relatively low (~130 °C), which limits its potential in high-power applications. To address this issue, a new piezoelectric single crystal material, PIN-PMN-PT, has been proposed and is being investigated for its higher Curie temperature [32]. In addition, the PMN-PN composite based PA/US imaging system can be further improved, including achieving higher resolution of PA/US images for visualizing the microvasculature of the rectum wall by using a single mode fiber and higher frequency ultrasonic transducer, and precise assembly of the imaging probe with help from 3D printing (printing resolutions: 10 μm for XY-axis and 25 μm for Z-axis). The improved performance of the PA/US transducer is a critical step to translate this technology to clinical application.

Author contributions

Z.C. and Q.Z. initiated this investigation, supervised the project, and edited the paper. Y.L. and G.L. implemented the project, analyzed the data and wrote the paper. C.J. and J.J. contributed to the data acquisition. T.H. contributed to the data analysis. R.C. and L.J. contributed to the preparation of piezoelectric materials and ultrasound transducers.

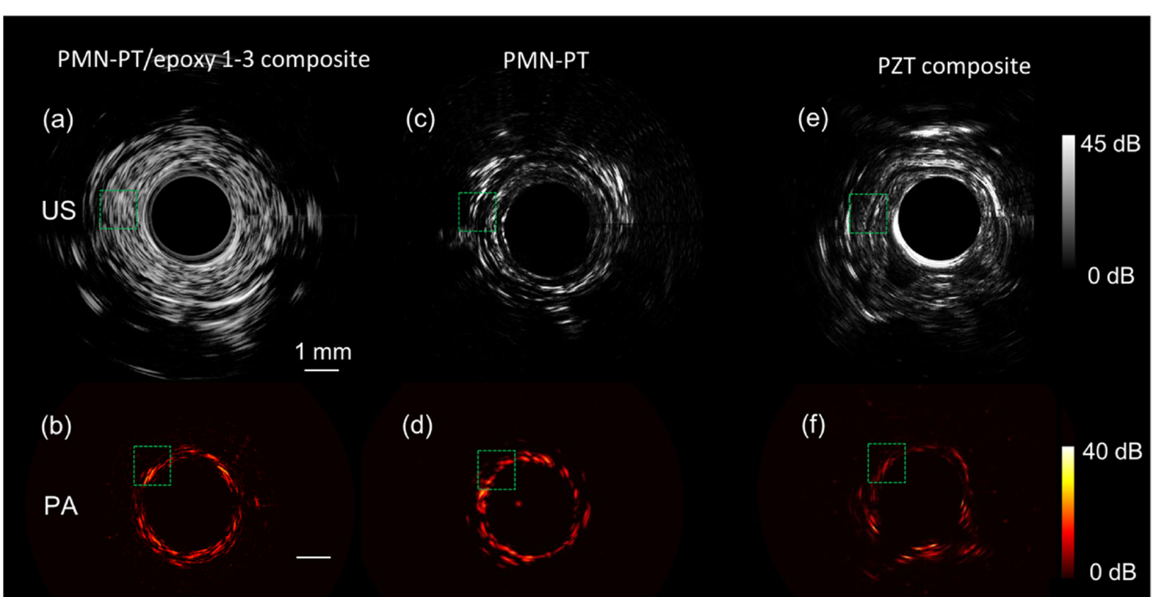

Fig. 4. US and PA images of *in vivo* imaging of rat rectum. (a) and (b): PMN-PT/epoxy 1–3 composite. (c) and (d): PMN-PT. (e) and (f): PZT composite.

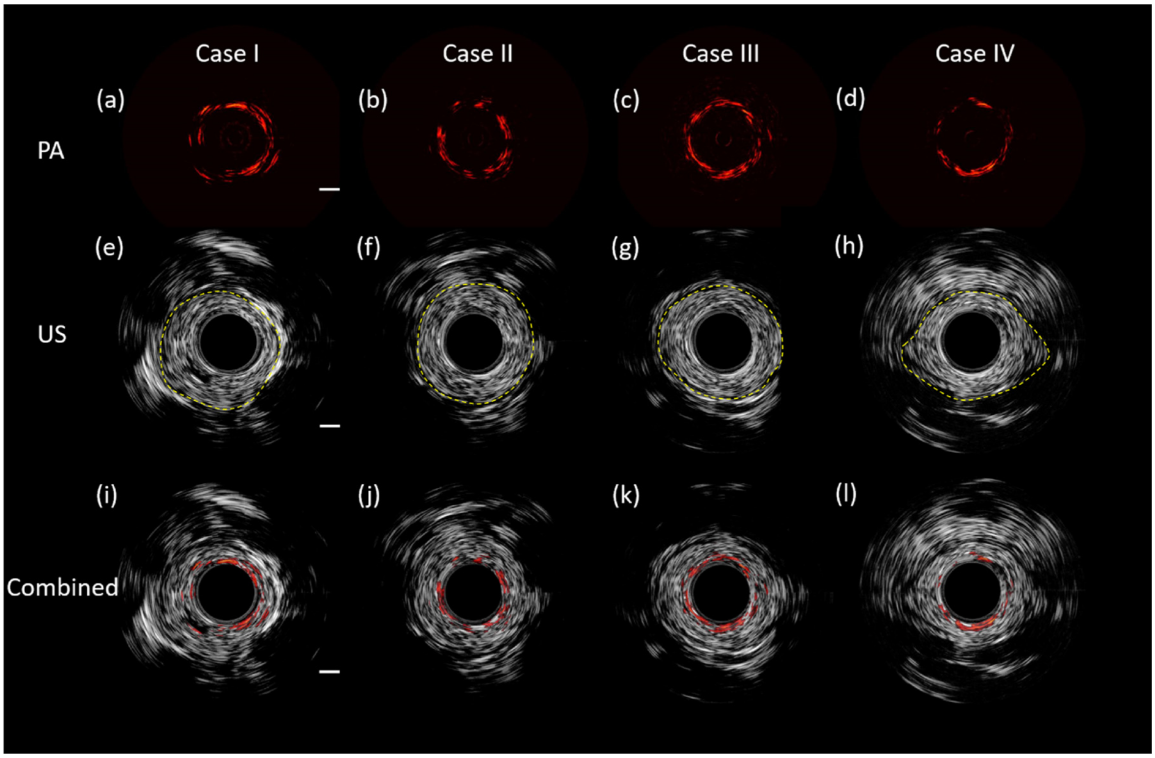

Fig. 5. PA, US, and combined images of *in vivo* imaging of rat rectum. (a–d): PA images. (e–h): US images. (i–l): combined PA and US images. Scale bar: 1 mm. Cases I, II, III, and IV: different longitudinal positions of rat rectum.

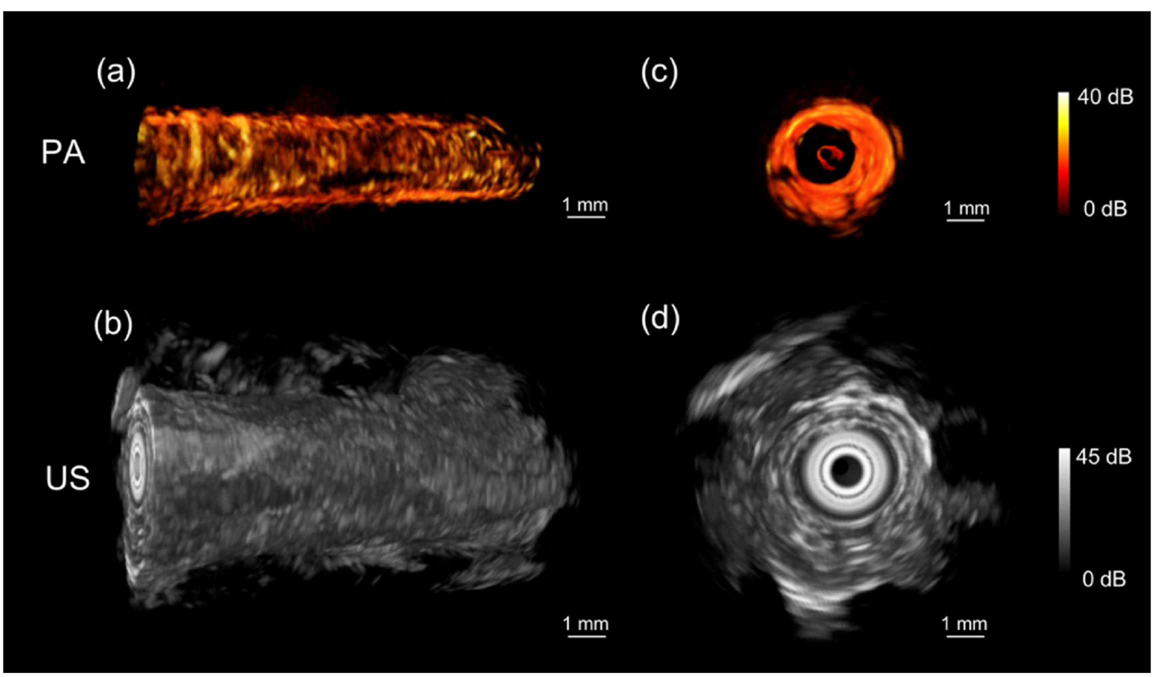

Fig. 6. 3D endoscopic PA and US images of the rat rectum. (a) and (c) 3D PA images. (b) and (d) 3D US images. Scale bar: 1 mm.

Funding

National Institutes of Health (R01HL-125084, R01HL-127271, R01EY-026091, and R01EY-028662), American Heart Association (18PRE34050021), the National Science Foundation (DGE-1839285).

Declaration of Competing Interest

Dr. Chen has a financial interest in OCT Medical Imaging, Inc., which, however, did not support this work.

References

[1] J.M. Yang, K. Maslov, H.C. Yang, Q. Zhou, K.K. Shung, L.V. Wang, Photoacoustic endoscopy, Opt. Lett. 34 (10) (2009) 1591–1593.

[2] L.V. Wang, Photoacoustic Imaging and Spectroscopy, Taylor & Francis/CRC Press, Boca Raton, Florida, 2009.
[3] G. Ku, B.D. Fornage, X. Jin, M. Xu, K.K. Hunt, L.V. Wang, Thermoacoustic and photoacoustic tomography of thick biological tissues toward breast imaging, Technol. Cancer Res. Treat. 4 (5) (2005) 559–566.
[4] R. Ansari, E.Z. Zhang, A.E. Desjardins, P.C. Beard, All-optical forward-viewing photoacoustic probe for high-resolution 3D endoscopy, Light Sci. Appl. 7 (2018) 75.
[5] S.J. Mathews, C. Little, C.D. Loder, R.D. Rakhit, W. Xia, E.Z. Zhang, P.C. Beard, M.C. Finlay, A.E. Desjardins, All-optical dual photoacoustic and optical coherence tomography intravascular probe, Photoacoustics 11 (2018) 65–70.
[6] G. Wissmeyer, M.A. Pleitez, A. Rosenthal, V. Ntziachristos, Looking at sound: optoacoustics with all-optical ultrasound detection, Light Sci. Appl. 7 (2018) 53.
[7] Z. Chen, S. Yang, Y. Wang, D. Xing, Noncontact broadband all-optical photoacoustic microscopy based on a low-coherence interferometer, Appl. Phys. Lett. 106 (4) (2015).
[8] Z. Guo, G. Li, S.L. Chen, Miniature probe for all-optical double gradient-index lenses photoacoustic microscopy, J. Biophotonics 11 (12) (2018) e201800147.
[9] G. Li, Z. Guo, S.L. Chen, Miniature all-optical probe for large synthetic aperture photoacoustic-ultrasound imaging, Opt. Express 25 (21) (2017) 25023–25035.
[10] C. Sheaff, S. Ashkenazi, An all-optical thin-film High-frequency ultrasound transducer, Ieee International Ultrasonics Symposium (Ius) (2011), (2011), pp. 1944–1947.
[11] S. Preisser, W. Rohringer, M. Liu, C. Kollmann, S. Zotter, B. Fischer, W. Drexler, All-optical highly sensitive akinetic sensor for ultrasound detection and photoacoustic imaging, Biomed. Opt. Express 7 (10) (2016) 4171–4186.
[12] Y. Li, X. Gong, C. Liu, R. Lin, W. Hau, X. Bai, L. Song, High-speed intravascular spectroscopic photoacoustic imaging at 1000 A-lines per second with a 0.9-mm diameter catheter, J. Biomed. Opt. 20 (6) (2015) 065006.
[13] Y. Li, R. Lin, C. Liu, J. Chen, H. Liu, R. Zheng, X. Gong, L. Song, In vivo photoacoustic/ultrasonic dual-modality endoscopy with a miniaturized full field-of-view catheter, J. Biophotonics 11 (10) (2018) e201800034.
[14] M. Abran, G. Cloutier, M.H. Cardinal, B. Chayer, J.C. Tardif, F. Lesage, Development of a photoacoustic, ultrasound and fluorescence imaging catheter for the study of atherosclerotic plaque, IEEE Trans. Biomed. Circuits Syst. 8 (5) (2014) 696–703.
[15] Y. Cao, J. Hui, A. Kole, P. Wang, Q. Yu, W. Chen, M. Sturek, J.X. Cheng, High-sensitivity intravascular photoacoustic imaging of lipid-laden plaque with a collinear catheter design, Sci. Rep. 6 (2016) 25236.
[16] Z. Guo, Y. Li, S.L. Chen, Miniature probe for in vivo optical- and acoustic-resolution photoacoustic microscopy, Opt. Lett. 43 (5) (2018) 1119–1122.
[17] J.M. Yang, R. Chen, C. Favazza, J. Yao, C. Li, Z. Hu, Q. Zhou, K.K. Shung, L.V. Wang, A 2.5-mm diameter probe for photoacoustic and ultrasonic endoscopy, Opt. Express 20 (21) (2012) 23944–23953.
[18] A.B. Karpiouk, B. Wang, S.Y. Emelianov, Development of a catheter for combined intravascular ultrasound and photoacoustic imaging, Rev. Sci. Instrum. 81 (1) (2010) 014901.
[19] J. Hui, Y. Cao, Y. Zhang, A. Kole, P. Wang, G. Yu, G. Eakins, M. Sturek, W. Chen, J.X. Cheng, Real-time intravascular photoacoustic-ultrasound imaging of lipid-laden plaque in human coronary artery at 16 frames per second, Sci. Rep. 7 (1) (2017) 1417.
[20] M. Wu, A.F.W. van der Steen, E. Regar, G. van Soest, Emerging technology update intravascular photoacoustic imaging of vulnerable atherosclerotic plaque, Interv Cardiol 11 (2) (2016) 120–123.
[21] J.M. Yang, C. Li, R. Chen, Q. Zhou, K.K. Shung, L.V. Wang, Catheter-based photoacoustic endoscope, J. Biomed. Opt. 19 (6) (2014) 066001.
[22] J.M. Yang, C. Favazza, R. Chen, J. Yao, X. Cai, K. Maslov, Q. Zhou, K.K. Shung, L.V. Wang, Simultaneous functional photoacoustic and ultrasonic endoscopy of internal organs in vivo, Nat. Med. 18 (2012) 1297–1302.
[23] J.M. Yang, C. Li, R. Chen, B. Rao, J. Yao, C.H. Yeh, A. Danielli, K. Maslov, Q. Zhou, K.K. Shung, L.V. Wang, Optical-resolution photoacoustic endomicroscopy in vivo, Biomed. Opt. Express 6 (3) (2015) 918–932.
[24] K. Jansen, M. Wu, A.F. van der Steen, G. van Soest, Photoacoustic imaging of human coronary atherosclerosis in two spectral bands, Photoacoustics 2 (1) (2014) 12–20.
[25] X. Bai, X. Gong, W. Hau, R. Lin, J. Zheng, C. Liu, C. Zeng, X. Zou, H. Zheng, L. Song, Intravascular optical-resolution photoacoustic tomography with a 1.1 mm diameter catheter, PLoS One 9 (3) (2014) e92463.
[26] D. VanderLaan, A.B. Karpiouk, D. Yeager, S. Emelianov, Real-time intravascular ultrasound and photoacoustic imaging, IEEE Trans. Ultrason. Ferroelectr. Freq. Control 64 (1) (2017) 141–149.
[27] Q. Zhou, K.H. Lam, H. Zheng, W. Qiu, K.K. Shung, Piezoelectric single crystals for ultrasonic transducers in biomedical applications, Prog. Mater. Sci. 66 (2014) 87–111.
[28] Q. Zhou, E.L. Gottlieb, L. Sun, L.M. Cannata, H. Ameri, M.S. Humayun, H. Pengdi, K.K. Shung, PMN-PT single crystal, high-frequency ultrasonic needle transducers for pulsed-wave Doppler application, IEEE Trans. Ultrason., Ferroelect., Freq. Contr. 54 (2007) 668–675.
[29] G.Z. Cao, Qing Guo, I.Y. Shen, Measurements of piezoelectric coefficient d33 of lead zirconate titanate thin films using a mini force hammer, J. Vib. Acoust. 135 (1) (2013).
[30] K.B. Kim, D.K. Hsu, B. Ahn, Y.G. Kim, D.J. Barnard, Fabrication and comparison of PMN-PT single crystal, PZT and PZT-based 1-3 composite ultrasonic transducers for NDE applications, Ultrasonics 50 (8) (2010) 790–797.
[31] K.K. Shung, J.M. Cannata, Q.F. Zhou, Piezoelectric materials for high frequency medical imaging applications: a review, J. Electroceramics 19 (1) (2007).
[32] P. Sun, Q.F. Zhou, B.P. Zhu, D.W. Wu, C.L. Hu, J.M. Cannata, J. Tian, P.D. Han, G.F. Wang, K.K. Shung, Design and fabrication of PIN-PMN-PT single-crystal high-frequency ultrasound transducers, IEEE Trans. Ultrason. Ferroelectr. Freq. Control 56 (12) (2009) 2760–2763.

Yan Li received the B.S. and M.S. degrees from the Tianjin University and Changchun Institute of Optics, Fine Mechanics and Physics, Chinese Academy of Science, Beijing, China, in 2011 and 2014, respectively. She is currently working toward the Ph.D. degree under the guidance of Dr. Zhongping Chen. Her research interests include multimodality endoscopic imaging by combining ultrasonic and optical techniques, such as ultrasound, optical coherence tomography, photoacoustic imaging, and fluorescence.

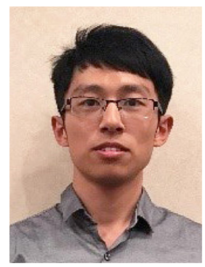

Gengxi Lu received his bachelor's degree in Physics from Nanjing University, China, in 2017. He is currently a Ph.D. student at the Department of Biomedical Engineering, University of Southern California, Los Angeles, CA, USA. His research interests include the development of intravascular ultrasound transducers, photoacoustics, ophthalmology and acoustic metamaterials.

Jason J. **Chen** received the bachelor's degree from the University of California, Irvine, CA, USA, in 2013. He worked as a Research Specialist for Dr. Brian J.F. Wong at the Beckman Laser Institute, University of California, Irvine, CA, USA, until he started the Ph.D. program in 2017. His research interests include optical coherence tomography, including optical system design, software analysis, and applications in otolaryngology and ophthalmology

Joseph C. Jing received the Ph.D. degree from the Department of Biomedical Engineering, University of California, Irvine, CA, USA, in 2016. He is currently working as a Postdoctoral Scholar with the Department of Medical Engineering, Caltech, Pasadena, CA, USA. His research interest includes the development of novel high-speed imaging technologies for *in vivo* biomedical applications.

Tiancheng Huo received a Ph.D degree in Physics from Tsinghua University, China, in 2015. His interest includes optical coherence tomography, high speed swept-source laser, ultrafast analog photonic signal processing, space-variant polarized beams, orbital angular momentum-carrying femtosecond laser, multidimensional total E-field reconstructions technique and the spectral domain ghost imaging.

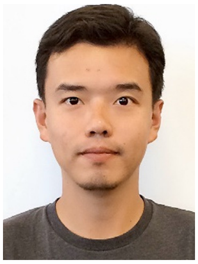

Laiming Jiang received his B.S. degree in Materials Science and Engineering from Sichuan University, China, in2013. He is currently a joint Ph.D. student from Keck School of Medicine at University of Southern California, Los Angeles, CA and the College of Materials Science and Engineering, Sichuan University, Sichuan, China. His current research interests include the development of lead-free piezoelectric materials and flexible ultrasonic devices.

Ruimin Chen received his B.S. degree in Biomedical Engineering from University of Electronics Science and Technology of China, Chengdu, China in 2006, and both his M.S. and his Ph.D. degrees in Biomedical Engineering from University of Southern California, Los Angeles, CA, in 2008 and 2014, respectively. He is currently a postdoctoral research associate and resource manager in the NIH Resource Center for Medical Ultrasonic Transducer Technology at the Department of Biomedical Engineering of University of Southern California. His research interests include the design, modeling, and fabrication of high-frequency ultrasonic transducers and arrays for medical imaging applications, piezoelectric material characterization, and photoacoustic imaging.

Qifa Zhou received the Ph.D. degree from the Department of Electronic Materials and Engineering, Xi'an Jiaotong University, Xi'an, China, in 1993. He is currently working as a Research Professor with the NIH Resource on Medical Ultrasonic Transducer Technology and the Department of Biomedical Engineering and Industry and System Engineering, University of Southern California (USC), Los Angeles, CA, USA. Before joining USC in 2002, he worked in the Department of Physics, Zhongshan University in China, the Department of Applied Physics, Hong Kong Polytechnic University, and the Materials Research Laboratory, Pennsylvania State University. His current research interests include the development of ferroelectric thin films, MEMS technology, nano-composites, and modeling and fabrication of high-frequency ultrasound transducers and arrays for medical imaging applications, such as photoacoustic imaging and intravascular imaging. He has published more than 130 journal papers in this area. Dr. Zhou is a fellow of the International Society for Optics and Photonics and the American Institute for Medical and Biological Engineering. He is also a senior member of the IEEE Ultrasonics, Ferroelectrics, and Frequency Control (UFFC) Society and a member of the UFFC Society's Ferroelectric Committee. He is a member of the Technical Program Committee of the IEEE International Ultrasonics Symposium. He is an Associate Editor of the IEEE Transactions on Ultrasonics, Ferroelectrics, and Frequency Control.

Zhongping Chen received the B.S. degree in applied physics from Shanghai Jiao Tong University, Shanghai, China, in 1982, the M.S. degree in electrical engineering and the Ph.D. degree in applied physics both from the Cornell University, Ithaca, NY, USA, in 1987 and 1993, respectively. He is currently working as a Professor of biomedical engineering and the Director of the F-OCT Laboratory at the University of California, Irvine, CA, USA. He is co-founder and Board Chairman of OCT Medical Imaging, Inc., Irvine, CA. His research interests include the areas of biomedical photonics, microfabrication, biomaterials, and biosensors. His research group has pioneered the development of functional optical coherence tomography, which simultaneously provides high-resolution three-dimensional images of tissue structure, blood flow, and birefringence. He has published more than 220 peer-reviewed papers and review articles and holds a number of patents in the fields of biomaterials, biosensors, and biomedical imaging. Dr. Chen is a Fellow of the American Institute of Medical and Biological Engineering, a Fellow of SPIE, and a Fellow of the Optical Society of America.